Luminescent graphene-based materials via europium complexation on dipyridylpyridazine-functionalized graphene sheets

Juan Amaro-Gahete,[a] Anna M. Kaczmarek,*[b] Dolores Esquivel,*[a] César Jiménez-Sanchidrián,[a] Pascal Van Der Voort,[b] and Francisco J. Romero-Salguero*[a]

Dedicated to Prof. Jean-Marie Lehn on the occasion of his 80th birthday

Abstract: Graphene-based materials exhibit outstanding physical properties and so are potentially applicable in a great variety of fields. Unlike their corresponding oxides, graphite and graphene are not prone to functionalization. Diels-Alder reactions are among the scarce reactions that they can undergo without disrupting their conjugated sp^2 systems. Herein, the reaction between graphite and 3,6-di(2-pyridyl)-1,2,4,5-tetrazine under different conditions affords several graphene-based materials consisting of dipyridylpyridazine functionalized few layer graphene, multilayer graphene and graphite whose sheets act as ligands for the grafting of a europium complex. These three materials show strong red emission under 365 nm UV radiation. Their emitting particles can be visualized by confocal microscopy. The rich coordination chemistry of dipyridylpyridazine ligands envisages novel properties for similarly functionalized graphene-based materials grafted with other metal complexes.

Introduction

Graphene-based materials will have an outstanding technological impact in the future in virtue of their availability and excellent mechanical, thermal, electrical and electronic properties. The possibility to impart them with photonic properties is challenging and will be of a high interest. Emitting nanomaterials have potential applications in many areas, including sensing, bioimaging and photocatalysis, among others.[1] However, graphene is a zero band gap semiconductor and so practically it does not exhibit any luminescence.[2]

At present there are two general strategies to produce luminescent graphene-based materials.[3] The first one involves the existence of sp^2 isolated islands without π connections, as occurs in some reduced graphene oxides. The second one originates from the presence of defects, as occurs in carbon quantum dots. These nanomaterials exhibit emissions that are concentrated in the blue and green regions.

Previous strategies are basically based on the introduction of defects in the graphene sheets and so unavoidably will lead to materials with depleted properties.

3,6-Di(2-pyridyl)pyridazine units have received great attention as ligands for coordination and supramolecular chemistry.[4] These ligands can be synthesized by an inverse electron demand Diels−Alder reaction between the corresponding 3,6-di(2-pyridyl)-1,2,4,5-tetrazine (as diene) and alkynes or alkenes (as dienophiles).[5]

Hybrid materials have also been functionalized through hetero Diels-Alder reactions. Thus, in recent years, the emission properties of different organosilicas via their functionalization with lanthanide complexes via surface dipyridylpyridazine ligands have been explored. These surface adducts were generated by Diels-Alder reaction between C=C double bonds in the organosilica (dienophile) and 3,6-di(2-pyridyl)-1,2,4,5-tetrazine (diene). In particular, these surface adducts were proven to be suitable sensitizing ligands for europium ions,[6] provided hybrid near-infrared (NIR) emitting materials upon complexation with NIR emitting lanthanide ions (Nd^{3+}, Er^{3+}, Yb^{3+})[7] and a luminescent optical thermometer when grafted with Eu^{3+}/Tb^{3+} ions.[8]

Nitrogen-doped graphenes can be obtained by two general strategies, i.e. direct synthesis and posttreatment. Regardless of the doping procedure, different nitrogen types at different locations are generated and so specific sites for metal coordination are ill-defined.[9]

Haddon et al.[10,11] have reported that both graphite and graphene can act as dienes and dienophiles in the Diels-Alder reaction. Particularly, their behavior as dienophiles was investigated using 9-methylanthracene, 9,10-dimethylanthracene and 2,3-dimethoxy-1,3-butadiene, all of them electron-rich dienes. A later computational study revealed that these cycloaddition reactions did not take place in the inner bonds of graphene but in its edges.[12]

Recently, Schirrmacher et al.[13] have demonstrated the effectiveness of the Diels-Alder reaction with a carbonaceous matrix material and a tetrazine-based compound functionalizing single-walled carbon nanotubes with 3,6-dichlorotetrazine conjugated to Au nanoparticles. Similarly, they reported later the Diels-Alder reaction between substituted chlorotetrazines and HOPG under mild conditions.[14]

Considering that dipyridylpyridazine derivatives are excellent ligands for the coordination of different metals and the exciting

[a] J. Amaro-Gahete, Prof. D. Esquivel, Prof. C. Jiménez-Sanchidrián, Prof. F. J. Romero-Salguero.
Departamento de Química Orgánica, Instituto Universitario de Nanoquímica de la Universidad de Córdoba IUNAN.
Facultad de Ciencias, Universidad de Córdoba.
Campus de Rabanales, Ed. Marie Curie, E-14071 Córdoba, Spain.
E-mail: go2rosaf@uco.es, g12esmem@uco.es

[b] Prof. A.M. Kaczmarek, Prof. P. Van Der Voort
COMOC, Department of Chemistry
Ghent University
Krijsglaan 281-S3, B-9000 Ghent, Belgium
E-mail: Anna.Kaczmarek@UGent.be

Supporting information for this article is given via a link at the end of the document.

applications of Ln grafted materials, herein we have prepared dipyridylpyridazine (dppz) graphene-based materials, which subsequently have been used for the coordination of europium complexes as examples of visible emitting lanthanide ions.

Results and Discussion

Synthesis and characterization of dipyridylpyridazine graphene-based materials

A screening of the Diels-Alder reaction between graphene-based materials and 3,6-di(2-pyridyl)tetrazine was carried out under a variety of conditions (Tables S1-S3). The degree of functionalization, measured as the N content, varied with the substrate, activation of the reaction and time. Broadly, the reactivity of the graphene-derived materials decreased in the following order: graphene nanosheets > micrographite > graphite > multiwalled carbon nanotubes. These results agree with the preferential functionalization of the double bonds located at the edges of the graphene sheets, as proposed by Houk et al.[12] Accordingly, a microcrystalline graphite powder was selected as starting material.

Three materials were synthesized by three different reaction procedures (see Experimental section): one-pot ultrasound-assisted exfoliation and functionalization (dppz-FLG); dry mechanochemical reaction (dppz-MLG); and refluxing (dppz-MG). When a tetrazine is used as an electron-deficient diene, the Diels-Alder cycloaddition is subsequently followed by a retro-Diels-Alder reaction with N_2 release, giving rise to a dihydropyridazine adduct (Scheme 1). This adduct can be dehydrogenated to the corresponding pyridazine with different oxidizing agents. In this work, DDQ was used after the Diels-Alder reactions. As many of these reagents can also participate in oxidative cyclodehydrogenation reactions,[15] the dppz units could be bound to the graphene sheet in different ways, which otherwise are indistinguishable. Elemental analysis of the three samples gave N contents of 3.5, 4.1 and 1.6 wt% for dppz-FLG, dppz-MLG and dppz-MG, respectively.

Raman spectroscopy confirmed the functionalization of graphene sheets in the three materials (Figure 1). The intensity ratio of the D and G bands (I_D / I_G) has been related to the degree of disorder corresponding to the effective functionalization in the Diels-Alder reaction.[10] In all cases, the I_D / I_G ratio increased for the functionalized materials, from 0.10 for the parent micrographite to ca. 1.0 for the dppz-MLG sample. Raman spectroscopy is also a useful technique to determine the number of sheets in graphene-based materials. Two procedures were selected and applied to unfunctionalized and dppz-functionalized materials (see SI). Equation S1 provided 7 and 15 layers for FLG and MLG materials, whereas equation 2 gave 9 and 11 layers, respectively.[16,17] Concerning the functionalized materials, dppz-FLG and dppz-MLG presented a number of 5 and 12 layers according to equation 1 and 10 and 13 according to equation S3. As a consequence, the material obtained by the ultrasound method can be considered as a few layer graphene whereas that synthesized by a mechanochemical procedure can be classified as a multilayer graphene.[18] The mechanochemical exfoliation of graphite has been reported previously. For example, ball-milling of graphite with melamine has been used for the production of few-layer graphenes.[19]

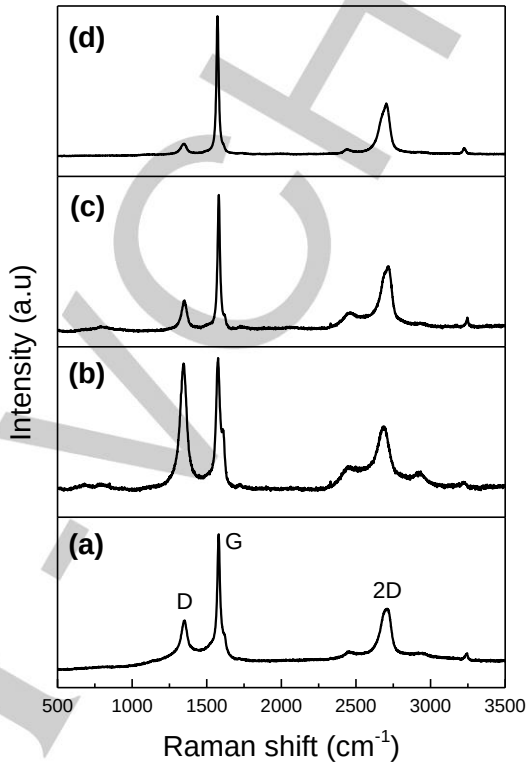

Figure 1. Raman spectra of materials (a) dppz-FLG, (b) dppz-MLG, (c) dppz-MG and (d) the parent MG.

The parent graphite and the functionalized materials were examined by TEM images. The original graphite showed a multilayered structure composed of numerous individual graphene sheets (Figure 2-a). A similar structure was observed for the material functionalized by a refluxing procedure dppz-MG (Figure 2-d).

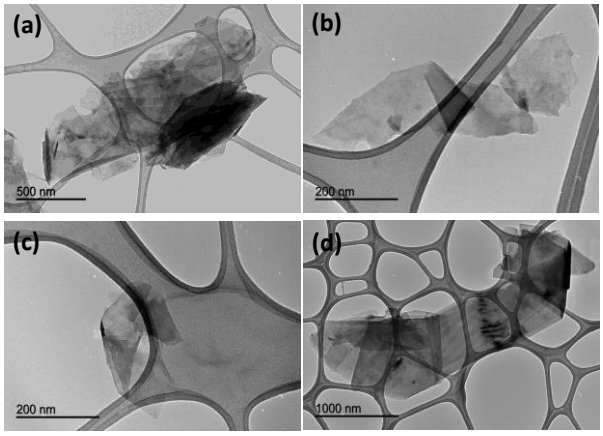

Figure 2. TEM images of the three functionalized materials (a) dppz-FLG, (b) dppz-MLG and (c) dppz-MG.

Scheme 1. Hetero Diels-Alder reaction between graphene sheets and 3,6-di(2-pyridyl)tetrazine.

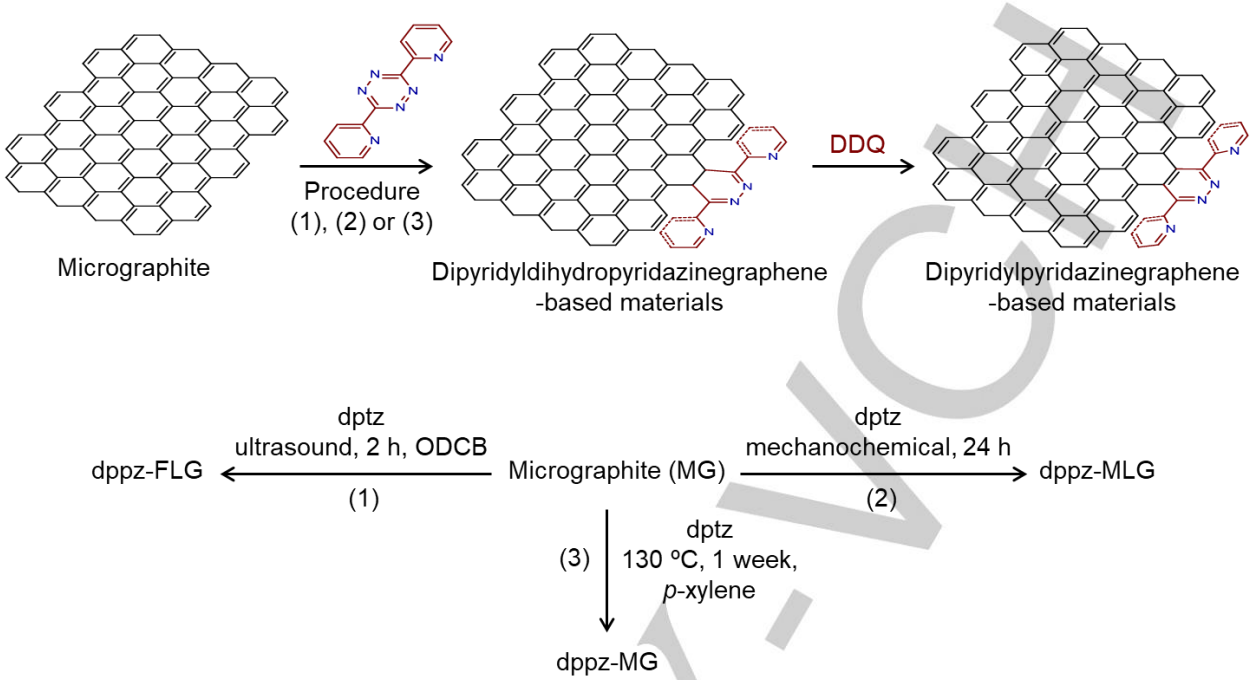

Unlike, TEM images of dppz-FLG and dppz-MLG materials (Figure 2-b and 2-c) revealed the presence of transparent thin sheets resulting from stacking of exfoliated layers, less in the former than in the latter material.

The functionalization of these materials was also confirmed by performing X-ray photoelectron spectroscopy (Figure 3). The charging effect has been corrected by taking the adventitious carbon to 284.8 eV as a reference. The N1s signal of 3,6-di(2-pyridyl)-1,2,4,5-tetrazine has been decomposed into two main components centered at 398.7 eV and 400.2 eV, corresponding to N in the pyridine and the tetrazine rings, respectively.[20] In order to ascertain the changes in the N1s signal upon formation of the adduct, a model compound, i.e. phenyl-3,6-di(2-pyridyl)pyridazine, was synthesized by Diels-Alder reaction between 3,6-di(2-pyridyl)-1,2,4,5-tetrazine and phenyl acetylene.[21] This compound only gave a N1s component at 399.2 eV, thus indicating that nitrogen in the pyridine and the pyridazine rings have the same signal, in agreement with Miomandre et al.[22] However, these authors suggested that the signal at higher binding energy separated by 1.4 eV was due to the N in the dihydropyridazine ring obtained by the Diels-Alder reaction between the tetrazine ring and the inner double bonds in the graphene sheets, which cannot be oxidized. Nevertheless, according to our results, the presence of two N1s signals separated by ca. 1.4 eV would be indicative of the presence of a tetrazine ring.

XPS spectra of the three functionalized materials, i.e. dppz-FLG, dppz-MLG and dppz-MG, exhibited a N1s signal close to 400 eV, thus confirming the incorporation of nitrogen in the three samples. The small shift toward higher binding energy with respect to the model pyridazine can be explained by the uncertainty of giving the same reference binding energy to the sp^2 carbon atoms in both graphene derivatives and heterocyclic compounds, the latter being affected by the presence of electronegative N atoms.

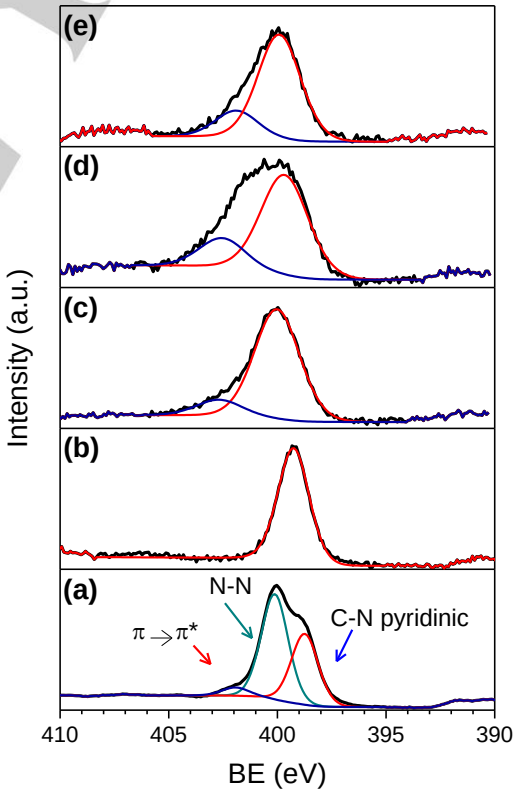

Figure 3. XPS spectra for the N1s photoemission peak of a) 3,6-di(2-pyridyl)-1,2,4,5-tetrazine, b) phenyl-3,6-di(2-pyridyl)pyridazine, c) dppz-FLG, d) dppz-MLG and e) dppz-MG.

In any case, this signal only contained one contribution and so it can be attributed to the formation of the dipyridylpyridazine adducts on the edges of the graphene sheets.
Additionally, all materials showed a band between 402-404.2 eV associated with the so-called π-π* transitions, characteristics of aromatic structures or unsaturated bonds.[23,24]
C1s XPS spectra of the three materials (Figure S1) revealed a slight oxidation of the graphene sheets in dppz-MLG, unlike dppz-FLG and dppz-MG. A comparison with the non-functionalized materials obtained by analogous procedures indicated that the oxidation occurred during the mechanochemical treatment. By contrast, dppz-FLG and dppz-MG exhibited a similar oxidation level to the parent graphite.

Room temperature photoluminescence properties of dppz-FLG, dppz-MLG and dppz-MG.

The excitation and emission spectra as well as luminescence decay times of the as prepared graphene-based materials were recorded and studied in detail. For the dppz-FLG material a broad band in the excitation spectrum was observed in the 250 – 350 nm range (Figure S2) When excited into the maximum of this band (280 nm), emission between 400 – 600 nm was observed with a maximum around 510 nm, showing emission in the green region (Figure S3). The luminescence decay profile of this sample could be well fitted using a monoexponential fit and yielded a decay time of 1.25 ns (Figure S4). For the dppz-MLG sample the excitation spectrum exhibited a broad band between 250 – 450 nm with a maximum at 375 nm (Figure S5). When excited at 375 nm an emission band with a maximum at 445 nm was observed, resulting in blue emission (Figure S6). The decay time for dppz-MLG could only be well fitted using a biexponential decay curve and yielded τ_1 = 1.51 ns and τ_2 = 6.53 ns (Figure S7). For the dppz-MG material the excitation and emission spectra were in a very similar range as that described for dppz-MLG (Figure S8 and S9). The decay time was recorded to be τ_1 = 1.55 ns and τ_2 = 6.26 ns (Figure S10) proving the dppz-MLG and dppz-MG materials to be very similar in their photoluminescence properties. All these values are similar to those reported in the literature for graphene oxides and reduced graphene oxides.[25]

Europium dipyridylpyridazine graphene complexes as visible emitters

Dipyridylpyridazinegraphene-based materials were used as ligands for the grafting of europium complexes (Scheme 2).
All the graphene-based materials were grafted with the $Eu(dbm)_3$ complex forming $Eu(dbm)_3$@dppz-FLG, $Eu(dbm)_3$@dppz-MLG and $Eu(dbm)_3$@dppz-MG materials. ICP-MS analysis revealed Eu contents of 1.6, 1.2 and 1.4 mmol g^{-1} for $Eu(dbm)_3$@dppz-FLG, $Eu(dbm)_3$@dppz-MLG and $Eu(dbm)_3$@dppz-MG, respectively. The $Eu(dbm)_3$ complex was used instead of a europium salt to ensure no (or a very low amount) water molecules in the first coordination sphere of the Eu^{3+} ions.
Additionally, the dbm ligand also works as a second antenna for the absorption of light making more efficient photoluminescence materials.

Scheme 2. Bis(dibenzoylmethane) europium complexes of dipyridylpyridazine graphene-based materials.

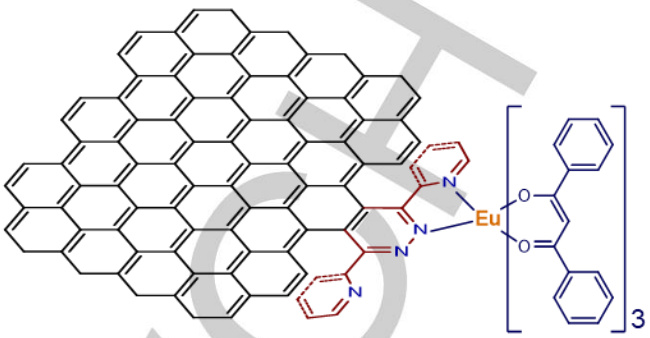

The coordination of $Eu(dbm)_3$ to dipyridylpyridazinegraphene-based materials was confirmed by Raman spectroscopy (Figure 4). The signal of Eu-O bond (v Eu-O= 405.1 cm^{-1}) was present in the $Eu(dbm)_3$ complex as well as in the three grafted materials, i.e. $Eu(dbm)_3$@dppz-FLG, $Eu(dbm)_3$@dppz-MLG and $Eu(dbm)_3$@dppz-MG. The binding of Eu ions to the N atoms in dipyridylpyridazinegraphene sheets was corroborated by the presence of a peak at 451.3 cm^{-1}.[26] The Eu-N bond was not observable in the case of the $Eu(dbm)_3$ complex. The parent MG showed no peaks in this Raman shift range.

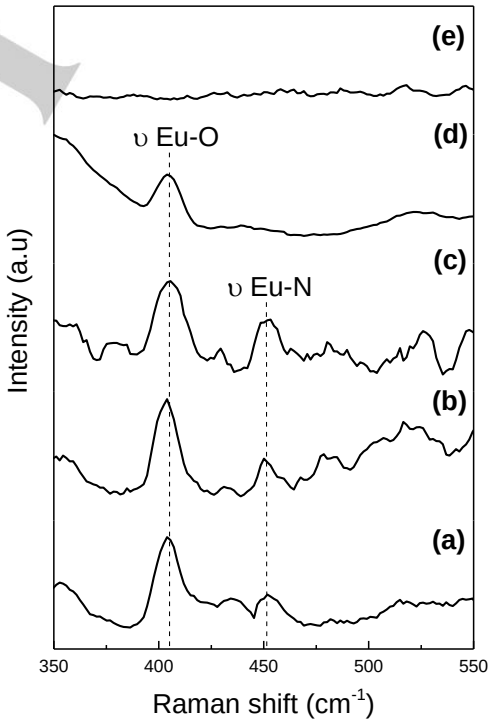

Figure 4. Raman spectra of materials (a) $Eu(dbm)_3$@dppz-FLG, (b) $Eu(dbm)_3$@dppz-MLG, (c) $Eu(dbm)_3$@dppz-MG, (d) $Eu(dbm)_3$ and (e) the parent MG.

The room temperature photoluminescence properties of the three materials were studied in detail – excitation and emission spectra, luminescence decay times and quantum yields. The combined excitation-emission spectrum of the pre-synthesized

$Eu(dbm)_3(H_2O)_2$ complex has been presented in Figure S11. The maximum of the excitation band was located around 400 nm and the characteristic $^5D_0 \rightarrow {}^7F_{0\text{-}4}$ transitions were observed in the emission spectrum. The decay time was calculated to be 0.338 ms (Figure S12). The recorded excitation and emission spectra of the $Eu(dbm)_3$@dppz-FLG, $Eu(dbm)_3$@dppz-MLG and $Eu(dbm)_3$@dppz-MG materials displayed quite similar photoluminescence properties. In the excitation spectra a broad band originating from the ligands can be observed between 250 – 425 nm, with a maximum around 390 nm. The samples could be excited at different wavelengths (320 nm, 350 nm and 390 nm) to yield the characteristic Eu^{3+} transition peaks: $^5D_0 \rightarrow {}^7F_0$ (577 nm), $^5D_0 \rightarrow {}^7F_1$ (591 nm), $^5D_0 \rightarrow {}^7F_2$ (611 nm), $^5D_0 \rightarrow {}^7F_3$ (651 nm) and $^5D_0 \rightarrow {}^7F_4$ (701 nm). The combined excitation-emission spectra for the $Eu(dbm)_3$@dppz-FLG material has been presented in Figure 5. The spectra for the $Eu(dbm)_3$@dppz-MLG and $Eu(dbm)_3$@dppz-MG materials have been presented in Figure S13 and S14. The luminescence decay times (excited into the maximum of the broad band) could only be well fitted using a biexponential equation, which suggests the presence of two different coordination environments of the Eu^{3+} ions in these materials. This could be a result of different binding modes to the dppz ligand or a different amount of dbm ligands and/or water molecules in the coordination environment. The decay times of the $Eu(dbm)_3$@dppz-FLG, $Eu(dbm)_3$@dppz-MLG and $Eu(dbm)_3$@dppz-MG materials have been overviewed in Table 1 and the decay profiles have been presented in Figure S15-S23.

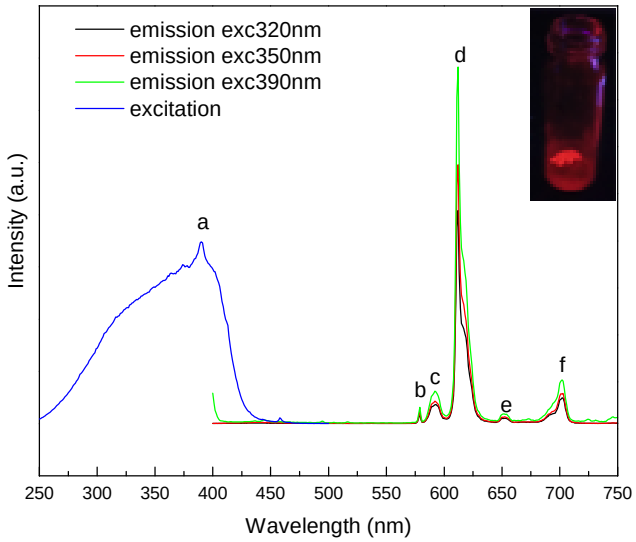

Figure 5. RT combined excitation-emission spectra for $Eu(dbm)_3$@dppz-FLG material. The excitation spectrum was observed at 611 nm. The labeled peaks are assigned to the following transitions: a (389.0 nm) – $\pi \rightarrow \pi^*$, b (579.0 nm) - $^5D_0 \rightarrow {}^7F_0$, c (591.0 nm) - $^5D_0 \rightarrow {}^7F_1$, d (612.0 nm) - $^5D_0 \rightarrow {}^7F_2$, e (651.0 nm) - $^5D_0 \rightarrow {}^7F_3$, f (702.0 nm) - $^5D_0 \rightarrow {}^7F_4$. The insert shows a photo of the sample under a laboratory UV lamp (365 nm excitation).

Despite the low QY values (presented in Table 1) the three materials showed strong red emission under 365 nm UV radiation with a laboratory UV lamp. Interestingly, these QY values are in the order of magnitude of those reported for most carbon quantum dots.[3]

Table 1. Luminescence decay times and quantum yields of the europium dipyridylpyridazine graphene complexes

Material	τ_1 (ms)	τ_2 (ms)	R^2	QY (%)
$Eu(dbm)_3$@dppz-FLG	0.209	0.065	0.999	2.8
$Eu(dbm)_3$@dppz-MLG	0.221	0.072	0.999	3.6
$Eu(dbm)_3$@dppz-MG	0.237	0.081	0.999	3.2

Some graphene-based materials have been visualized by direct fluorescence microscopy. In particular, GO nanosheets can be used as fluorescence labels but micron sized GO and reduced GO are unobservable in practice.[27] The strong fluorescence quenching of different dyes, such as fluorescein, by graphene-based materials has been used to visualize them by common fluorescence microscopy.[28]

The fluorescence imaging of graphitic materials by labeling is challenging, since the attached fluorophore will likely be quenched. In virtue of their interesting optical properties, the red emission of the Eu^{3+} complexes has been used to visualize these graphene-based materials by confocal microscopy. Material $Eu(dbm)_3$@dppz-FLG was observed both under dry conditions and dispersed in water (Figure 6). In both cases, particles with sizes between 300 and 600 nm were observable. Sample $Eu(dbm)_3$@dppz-MLG exhibited larger particles.

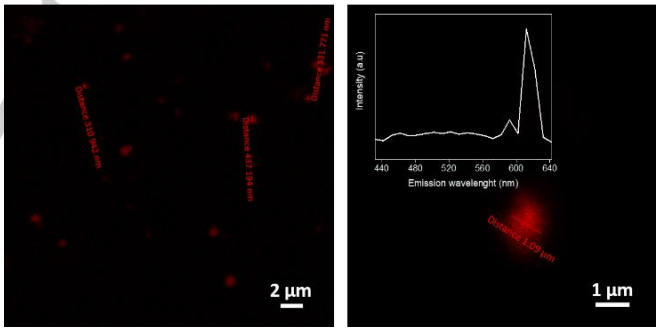

Figure 6. Images obtained by confocal microscopy of $Eu(dbm)_3$@dppz-FLG (left) and $Eu(dbm)_3$@dppz-MLG (right). The insert shown in the figure on the right represents the emission spectrum of a graphene particle determined by spectral image lambda stack from 427 to 668 nm with a resolution of 10 nm.

A spectral image lambda stack was gathered by the microscope for sample $Eu(dbm)_3$@dppz-MLG (Figure 6, inset). It provided a unique emission fingerprint that can be assigned to the graphene particle, thus revealing the sole contribution of this fluorophore to the sample emission.

In addition, material $Eu(dbm)_3$@dppz-FLG, which gives a stable dispersion in water, was subjected to tracking analysis (Figure 7). This technique allows to visualize and determine the size and concentration of nanoparticles.[29]

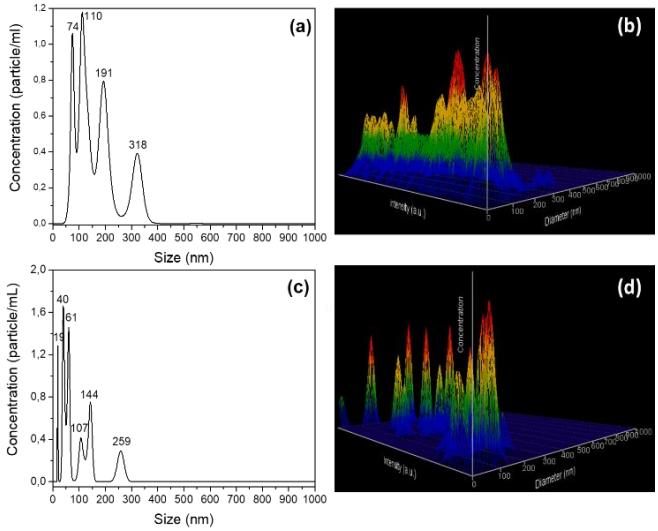

Figure 7. NTA analysis for Eu(dbm)$_3$@dppz-FLG in scatter mode ((a) and (b)) and fluorescence mode with excitation at 405 nm and a long pass filter at 430 nm ((c) and (d)).

A comparison of the scatter and fluorescence modes clearly indicated the formation of Eu^{3+} complexes in the graphene sheets since particles in the same range of sizes were observed in both cases, even though the fluorescence mode gave a higher resolution in the low size range, which can be caused by the differences in camera focus and capture and the non-spherical geometry of the particles. Interestingly, NTA would permit the selective visualization of graphene-based materials in complex media, which is essential for the study of the interaction of these nanomaterials with biological systems.

Conclusions

The hetero Diels-Alder reaction between 3,6-di(2-pyridyl)-1,2,4,5-tetrazine and graphene-based materials provides well-defined coordination sites for metal complexation on graphene sheets. Starting from the same graphite, three different procedures with alternative activation energy, i.e. ultrasounds, ball-milling and heating, resulted in dipyridylpyridazine derived few layer graphene, multilayer graphene and graphite. All of them have been proven to be useful ligands for complexation of europium. The emission properties of these materials have been studied before and after grafting with Eu(dbm)$_3$ complexes. It was observed that when exciting at a wide range of excitation wavelengths strong red emission of the Eu^{3+} could be observed. Grafting of the Eu^{3+} complex to graphene sheets has been unequivocally proven by Raman spectroscopy, nanoparticle tracking analysis and confocal microscopy, where emitting particles were clearly observable. Thus, this methodology allows to label graphene-based materials for bioimaging irrespective of their particle size.

In virtue of the interesting properties of lanthanide complexes, such as those for optics [30] and magnetism,[31] its combination with the outstanding graphene properties envisages the design and synthesis of new graphene-based materials with integrated properties for new applications.

In addition, the extension of this methodology to other graphene metal complexes can give materials with potential applications in organometallic chemistry, catalysis, biomedicine, imaging and sensing, among others.[32]

Experimental Section

Materials

Microcrystalline graphite (MG) powder (98 %) was purchased from Nanoestructured & amorphous materials Inc. 1,2-Dichlorobenzene (ODCB, anhydrous, 99%), dichloromethane (anhydrous, ≥99.8%, contains 40-150 ppm amylene as stabilizer), chloroform (anhydrous, ≥99%, contains 0.5-1.0% ethanol as stabilizer), 2-cyanopyridine (99%), hydrazine hydrate (reagent grade, N_2H_4 50-60 %), acetic acid (ReagentPlus, ≥99.99%), p-xylene (anhydrous, ≥99%), sodium nitrite (ACS reagent, ≥97.0%) and 2,3-dichloro-5,6-dicyano-p-benzoquinone (DDQ, 98%) were obtained from Sigma Aldrich. 3,6-Di(2-pyridyl)-1,2,4,5-tetrazine (dptz) and phenyl-3,6-di(2-pyridyl)pyridazine were synthesized by reported procedures.[7,21]

Methods

Synthesis of dppz-FLG

250 mg of microcrystalline graphite powder (MG) were added to a solution of 100 mg dptz in 50 mL of ODCB. The mixture was homogenized by stirring for 30 min. Then, the resulting dispersion was sonicated for 2 h (pulsed mode at 40% amplitude in an Ultrasonic Homogenizer 4710 Series from Cole Parmer Instrument Co.). The suspension obtained was centrifuged three times at 4000 rpm for 30 min to remove non-exfoliated graphite. The dispersion in ODCB was centrifuged at 10000 rpm for 30 min and the solid was washed five times with dichloromethane by successive redispersions and centrifugations. The resulting solid was dried under vacuum at 120 °C overnight. A dehydrogenation step was carried out with DDQ with a weight ratio solid:DDQ of 4:1 for 24 h using $CHCl_3$ as solvent. The dispersion was washed five times with dichloromethane by successive redispersions and centrifugations to eliminate excess of DDQ. The resulting solid, named dppz-FLG, was dried under vacuum at 120 °C overnight.

Synthesis of dppz-MLG

100 mg of microcrystalline graphite powder (MG) and 100 mg of dptz were introduced into the jar of a ball mill (Retsch PM100). The mixture was stirred for 24 h at 600 rpm with reversal of rotation every 30 min. The solid obtained was washed three times with dichloromethane: two with 25 mL at room temperature and one with 25 mL at 80 °C. After, the solid was dried at 120 °C under vacuum. A dehydrogenation step was carried out with DDQ with a weight ratio solid:DDQ 4:1 for 24 h using $CHCl_3$ as solvent. The dispersion was washed five times with dichloromethane by successive redispersions and centrifugations to eliminate excess of DDQ. The resulting solid, named dppz-MLG, was dried under vacuum at 120 °C overnight.

Synthesis of dppz-MG

A suspension of 100 mg of microcrystalline graphite powder (MG) and 100 mg of dptz in 10 mL of p-xylene was stirred for one week at 130 °C under a N_2 atmosphere. The solid was isolated by centrifugation at 4000 rpm. Subsequently, it was washed three times with dichloromethane: two with 25 mL at room temperature and one with 10 mL at 40 °C. Then, the solid was dried at 120 °C under vacuum. A dehydrogenation step was carried out with DDQ with a weight ratio solid:DDQ 4:1 for 24 h using $CHCl_3$ as solvent. The solid was washed five times with dichloromethane by successive redispersions and centrifugations to eliminate excess of DDQ. The resulting solid, named dppz-MG, was dried under vacuum at 120 °C overnight.

Synthesis of europium grafted dppz-FLG (Eu(dbm)$_3$@dppz-FLG; dbm = 1,3-Diphenyl, 1,3-propanedione)

For the preparation of Eu(dbm)$_3$@dppz-FLG a certain amount of presynthesized Eu(dbm)$_3$ complex (prepared according to previously reported procedure)[33] was dissolved in methanol in a Pyrex tube. Next, dppz-FLG in solid form was added to the lanthanide complex solution. This mixture was treated in an ultrasound bath for 30 min and left to soak at room temperature for the following 24 h. After this time, it was treated with ultrasound irradiation again for 30 min and next heated on a heating block for 24 h at 85 °C. After cooling down to room temperature the solid was collected on a glass filter, washed several times with methanol and left to dry in an oven at 50 °C.

Synthesis of europium grafted dppz-MLG (Eu(dbm)$_3$@dppz-MLG; dbm = 1,3-Diphenyl, 1,3-propanedione)

The synthesis of the Eu(dbm)$_3$@dppz-MLG materials was performed in a similar way as that described in 2.2.4. except dppz-MLG was used instead of dppz-FLG.

Synthesis of europium grafted dppz-MG (Eu(dbm)$_3$@dppz-MG; dbm = 1,3-Diphenyl, 1,3-propanedione)

The synthesis of the Eu(dbm)$_3$@dppz-MG materials was performed in a similar way as that described in 2.2.4. except dppz-MG was used instead of dppz-FLG.

Characterization of graphene-based materials

The nitrogen content was determined by elemental analysis in an Eurovector EA 3000. Transmission electron microscopy (TEM) images were recorded on a Jeol JEM-1400 transmission electron microscope operated at an accelerating voltage of 120 kV. The measurements have been made in a magnification range between 8,000x – 150,000x with an instrument resolution of 0.38 nm between points. Raman spectra were measured with a Renishaw Raman instrument (InVia Raman Microscope) by excitation with green laser light (532 nm). A total of 25 scans per spectrum were acquired to improve the signal-to-noise ratio. Raman spectroscopy was used to estimate the number of sheets in the graphitic materials (see SI) and to corroborate the coordination of the Eu complex with the nitrogen atoms present in the dppz-graphene/graphite matrix. XPS spectra were recorded on a SPECS mod. PHOIBOS 150 MCD spectrometer using monochromatic Mg Kα radiation and a multichannel detector. All spectra were fitted to Gauss–Lorentz curves. Eu(III) loadings in Eu(dbm)$_3$@dppz-graphene-based materials were determined by ICP-MS analysis in an ICP Mass Spectrometer model NexION^{TM} 350X, PerkinElmer Inc. 1 mg of Eu(dbm)$_3$@dppz-graphene-based materials was dissolved in a mixture of 200 µL of 69% HNO_3 (Merck, Suprapur), 50 µL of ≥30% H_2O_2 (Fluka, TraceSELECT@Ultra), 20 µl of 40% HF (Merck, Suprapur) and Milli-Q ultrapure water up to a total volume of 5 mL using an Ultrawave Single Reaction Chamber Microwave Digestion System, Milestone Inc. at 1500 W and temperature up to 220 °C. Confocal measurements were carried out in a ZEISS LSM 800 confocal microscope with oil immersion objective and equipped with 405 nm diode laser, MBS-405 nm filter and a gallium arsenide phosphide photomultiplier tube (GaAsP PMTs) as detector. One drop of an aqueous dispersion of the materials (1 mg of solid:3 mL of water) was placed on a microscope slide and subsequently protected with a cover slip. The edges of the protective glass were sealed with silicone. The lambda stack mode was selected to determine the emission spectrum of the fluorophore. NTA measurements were performed in a NanoSight NS300 (NanoSight, Malvern), equipped with a violet 405 nm laser and a 430 nm long pass filter. The minimum size limit of this technique is 10-40 nm. Luminescence measurements were performed on an Edinburgh Instruments FLSP920 UV-vis-NIR spectrometer setup. A 450 W xenon lamp was used as the steady-state excitation source. Time-resolved measurements were recorded using a 60 W pulsed Xe lamp operating at a frequency of 100 Hz (for visible emitting lanthanides). The very short decay times of the ungrafted dipyridylpyridazine graphene-based materials were measured using a Supercontinuum white light laser for TCSPC (Time Correlated Single Photon Counting). A Hamamatsu R928P photomultiplier tube was used to detect the emission signals in the near UV to visible range. All luminescence measurements were recorded at room temperature. Crystals were put between quartz plates (Starna cuvettes for powder samples, type 20/C/Q/0.2). For all of the compounds the luminescence decay curves were measured when excited into the broad ligand band (at different wavelengths) and monitored at the strongest europium transition. All of the decay curves could be well fitted using either a single exponential function or biexponential function.

$$I = A \exp\left(-\frac{t}{\tau}\right)$$

$$I = A_1 \exp\left(-\frac{t}{\tau_1}\right) + A_2 \exp\left(-\frac{t}{\tau_2}\right)$$

Where I represents the luminescence intensity and A, A_1 and A_2 are constants, t is time and τ, τ_1 and τ_2 are the luminescence lifetimes. All steady state and decay time measurements were performed with slit sizes of 1 nm (both excitation and emission) and a step size of 1 nm. The absolute overall quantum yields of the materials were measured by using an integrated sphere with a BENFLEC coating provided by Edinburgh Instruments as follows:

$$\eta = \frac{\int L_{\text{emission}}}{\int E_{\text{blank}} - \int E_{\text{sample}}}$$

where L_{emission} is the integrated value of the emission spectrum, and E_{blank} and E_{sample} are the integrated values of the "excitation" band of the blank and the excitation band of the sample (since the sample absorbs part of the light, this value will be smaller than E_{blank}), respectively.

Acknowledgements

The authors wish to acknowledge the financial support from Ramon Areces Foundation (Spain), Andalusian Regional Government (FQM-346 group), Spanish Ministry of Science, Innovation and Universities for an FPU teaching and research fellowship (FPU17/03981), Feder Funds and the technical staff from the Instituto Universitario de Investigación en Química Fina y Nanoquímica (IUIQFN) and Servicio Central de Apoyo a la Investigación (SCAI). A.M.K. acknowledges Ghent University for

funding and thanks Prof. Rik Van Deun for assess to the Edinburgh Instruments Spectrofluorometer in his lab.

Keywords: Graphene • N ligands • Cycloaddition • Lanthanides • Luminescence

[1] R. Wang, K.-Q. Lu, Z.-R. Tang, Y.-J. Xu, *J. Mater. Chem. A* **2017**, *5*, 3717–3734.

[2] X. Xu, C. Liu, Z. Sun, T. Cao, Z. Zhang, E. Wang, Z. Liu, K. Liu, *Chem. Soc. Rev.* **2018**, *47*, 3059–3099.

[3] S. Y. Lim, W. Shen, Z. Gao, *Chem. Soc. Rev.* **2015**, *44*, 362–381.

[4] M. Ruben, J. Rojo, F. J. Romero-Salguero, L. H. Uppadine, J.-M. Lehn, *Angew. Chemie Int. Ed.* **2004**, *43*, 3644–3662.

[5] R. Hoogenboom, G. Kickelbick, U. S. Schubert, *European J. Org. Chem.* **2003**, *2003*, 4887–4896.

[6] D. Esquivel, A. M. Kaczmarek, C. Jiménez-Sanchidrián, R. Van Deun, F. J. Romero-Salguero, P. Van Der Voort, *J. Mater. Chem. C* **2015**, *3*, 2909–2917.

[7] A. M. Kaczmarek, D. Esquivel, J. Ouwehand, P. Van Der Voort, F. J. Romero-Salguero, R. Van Deun, *Dalt. Trans.* **2017**, *46*, 7878–7887.

[8] A. M. Kaczmarek, D. Esquivel, B. Laforce, L. Vincze, P. Van Der Voort, F. J. Romero-Salguero, R. Van Deun, *Luminescence* **2018**, *33*, 567–573.

[9] H. Wang, T. Maiyalagan, X. Wang, *ACS Catal.* **2012**, *2*, 781–794.

[10] S. Sarkar, E. Bekyarova, S. Niyogi, R. C. Haddon, *J. Am. Chem. Soc.* **2011**, *133*, 3324–3327.

[11] S. Sarkar, E. Bekyarova, R. C. Haddon, *Acc. Chem. Res.* **2012**, *45*, 673–682.

[12] Y. Cao, S. Osuna, Y. Liang, R. C. Haddon, K. N. Houk, *J. Am. Chem. Soc.* **2013**, *135*, 17643–17649.

[13] J. Zhu, J. Hiltz, R. B. Lennox, R. Schirrmacher, *Chem. Commun.* **2013**, *49*, 10275–10277.

[14] J. Zhu, J. Hiltz, M. A. Mezour, V. Bernard-Gauthier, R. B. Lennox, R. Schirrmacher, *Chem. Mater.* **2014**, *26*, 5058–5062.

[15] L. P. Wijesinghe, S. D. Perera, E. Larkin, G. M. Ó Máille, R. Conway-Kenny, B. S. Lankage, L. Wang, S. M. Draper, *RSC Adv.* **2017**, *7*, 24163–24167.

[16] H. Wang, Y. Wang, X. Cao, M. Feng, G. Lan, *J. Raman Spectrosc.* **2009**, *40*, 1791–1796.

[17] K. R. Paton, E. Varrla, C. Backes, R. J. Smith, U. Khan, A. O'Neill, C. Boland, M. Lotya, O. M. Istrate, P. King, et al., *Nat. Mater.* **2014**, *13*, 624–630.

[18] S. Alwarappan, S. Boyapalle, A. Kumar, C.-Z. Li, S. Mohapatra, *J. Phys. Chem. C* **2012**, *116*, 6556–6559.

[19] V. León, M. Quintana, M. A. Herrero, J. L. G. Fierro, A. D. La Hoz, M. Prato, E. Vázquez, *Chem. Commun.* **2011**, *47*, 10936–10938.

[20] Y. Yamada, J. Kim, S. Matsuo, S. Sato, *Carbon N. Y.* **2014**, *70*, 59–74.

[21] S. Varughese, S. M. Draper, *Cryst. Growth Des.* **2010**, *10*, 2571–2580.

[22] Y. Li, G. Louarn, P.-H. Aubert, V. Alain-Rizzo, L. Galmiche, P. Audebert, F. Miomandre, *Carbon N. Y.* **2016**, *105*, 510–520.

[23] S. Biniak, G. Szymański, J. Siedlewski, A. Świątkowski, *Carbon N. Y.* **1997**, *35*, 1799–1810.

[24] S. Maldonado, S. Morin, K. J. Stevenson, *Carbon N. Y.* **2006**, *44*, 1429–1437.

[25] S. Vempati, T. Uyar, *Phys. Chem. Chem. Phys.* **2014**, *16*, 21183–21203.

[26] L. Jin, S. Lu, S. Lu, *Polyhedron* **1996**, *15*, 4069–4077.

[27] J. Kim, F. Kim, J. Huang, *Mater. Today* **2010**, *13*, 28–38.

[28] J. Kim, L. J. Cote, F. Kim, J. Huang, *J. Am. Chem. Soc.* **2010**, *132*, 260–267.

[29] S. Martins, J. P. S. Farinha, C. Baleizão, M. N. Berberan-Santos, *Chem. Commun.* **2014**, *50*, 3317–3320.

[30] J.-C. G. Bünzli, *Acc. Chem. Res.* **2006**, *39*, 53–61.

[31] D. N. Woodruff, R. E. P. Winpenny, R. A. Layfield, *Chem. Rev.* **2013**, *113*, 5110–5148.

[32] E. Bekyarova, S. Sarkar, S. Niyogi, M. E. Itkis, R. C. Haddon, *J. Phys. D. Appl. Phys.* **2012**, *45*, 154009.

[33] K. Binnemans, P. Lenaerts, K. Driesen, C. Görller-Walrand, *J. Mater. Chem.* **2004**, *14*, 191–195.

WILEY-VCH

Entry for the Table of Contents (Please choose one layout)

Layout 1:

FULL PAPER

Lighting graphene: Emitting graphene-based materials are obtained by complexation of europium compounds on dipyridylpyridazine moieties attached to their sheets via Diels-Alder reactions.

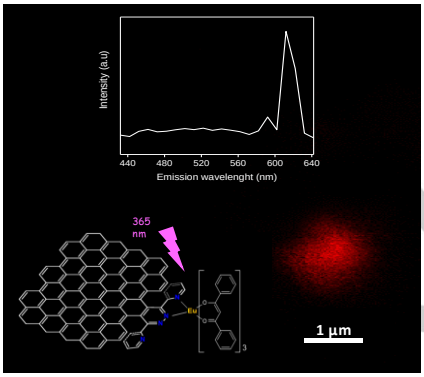

Juan Amaro-Gahete,[a] Anna M. Kaczmarek,[b] Dolores Esquivel,*[a] César Jiménez-Sanchidrián,[a] Pascal Van Der Voort,[b] and Francisco J. Romero-Salguero*[a]*

Page No. – Page No.

Luminescent graphene-based materials via europium complexation on dipyridylpyridazine-functionalized graphene sheets.

WILEY-VCH